Effects of Disorder on the Vibrational Properties of SiGe Alloys: Failure of Mean-Field Approximations

Stefano de Gironcoli and Stefano Baroni[a]
Institut Romand de Recherche Numérique en Physique des Matériaux (IRRMA), PHB-Ecublens, CH-1015 Lausanne, Switzerland
(Received 1 July 1992)

The vibrational properties of $Si_{1/2}Ge_{1/2}$ alloys are studied using *first principles* interatomic force constants. The effects of disorder are either simulated using large supercells or treated at the mean-field level by the coherent-potential approximation. The latter approach fails not only to reproduce the details of the Raman spectra due to the local atomic environment, but even to predict the three-mode behavior of this alloy. Supercell calculations, on the contrary, are in good agreement with observed Raman spectra and shed light on the microscopic mechanisms responsible for their detailed features.

PACS numbers: 63.50.+x

The vibrational properties of semiconductor alloys are currently the subject of active research both because of their intrinsic interest as realizations of simple disordered systems, and also because a detailed knowledge of the physical mechanisms governing them is a prerequisite for understanding the effects of disorder on the Raman spectra of semiconductor superlattices (SL's).

There are essentially two ingredients of any theoretical investigation of the vibrational properties of composite semiconductors such as SL's and alloys. The first is the knowledge of the *interatomic* force constants necessary to build up the dynamical matrix. The second is an appropriate scheme to treat the effects of disorder. By now, rather accurate real-space interatomic force constants are available from density-functional perturbation theory [1]. In those cases where the chemical disorder is weak and the composite system is unstrained—such as AlGaAs—the interatomic force constants of the virtual crystal provide a very accurate description of SL's and alloys [1(b),2,3]. This approach has been extended recently to the case of SiGe systems, where the contribution of microscopic strain to the actual force constants is nonnegligible, and the virtual-crystal approximation is therefore inadequate [4]. As for the effects of disorder, there are essentially two approaches for coping with them. In the first, substitutionally disordered systems are simulated by large, periodically repeated, unit cells (supercells, SC) where the actual atomic species at each lattice site is chosen at random. The vibrational properties are then obtained by averaging over several random configurations the results of straight diagonalization of the dynamical matrix which is calculated from the corresponding interatomic force constants and mass distribution. This approach is exact in principle, the only (nontrivial) limitation being the size of the SC necessary to simulate a macroscopic sample of material. In the second approach, the disorder is treated by introducing a periodic effective medium whose Green's function equals the *average* Green's function of the disordered system. In practice, the averaging process cannot be performed exactly, and one usually resorts to some kind of mean-field approximation, such as the average T-matrix approximation (ATA) [5], or the coherent-potential approximation (CPA) [6]. In these approaches, the displacement-displacement Green's function is considered—instead of the more physical displacement-momentum one—since with this choice the mass disorder appears as site diagonal.

Recently, mean-field approximations have been widely used to study the vibrational properties of various AlGaAs systems [7,8], and their results are in reasonable agreement with those of more sophisticated SC calculations [2,8]. In particular, the two-mode behavior of AlGaAs alloys as well as the dispersive character of phonons are well described within the CPA [7]. Also by virtue of this success, the CPA is currently being used to study the effects of disorder in SiGe superlattices [9]. In this paper we show that the CPA fails to predict not only some fine details of the vibrational spectrum of bulk $Si_{1/2}Ge_{1/2}$ which are due to the local atomic environment, but even its gross features—namely, its three-mode behavior. For this reason we expect that the CPA may fail badly in predicting the effects of disorder in SiGe superlattices, particularly in the frequency range where Si-Ge vibrations give an important contribution to the vibrational density of states, which is completely missing in the CPA picture. SC calculations, on the contrary, are in good agreement with experimental data and help to clarify the microscopic origin of even the fine details of the Raman spectra of the alloy. The failure of the CPA is analyzed by comparing its predictions for bulk $Si_{1/2}Ge_{1/2}$ alloys with "*exact*" results obtained from supercells of 512 atoms. All the SC spectral functions we present are averaged over six configurations and convoluted with a 2-cm^{-1}-wide Lorentzian to eliminate numerical noise. The Raman cross section has been calculated as in Refs. [2,4] by neglecting the different polarizabilities of the relevant atomic species. The interatomic force constants as well as other technical details are the same as in Ref. [4]. CPA calculations have been done using the virtual-crystal interatomic force constants and neglecting atomic

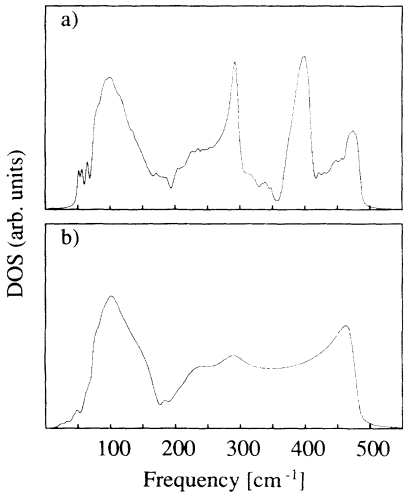

FIG. 1. Vibrational density of states of $Si_{1/2}Ge_{1/2}$ as obtained from (a) SC and (b) CPA calculations.

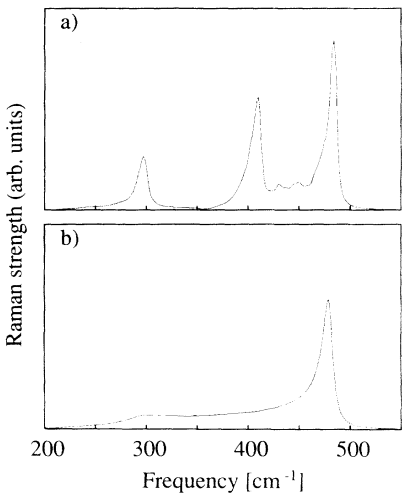

FIG. 2. Raman cross section of $Si_{1/2}Ge_{1/2}$ as obtained from (a) SC and (b) CPA calculations.

relaxation.

In Fig. 1 we compare the vibrational density of states (DOS) as obtained from SC calculations and from the CPA. The general features of the DOS is the acoustic region (below ≈ 250 cm^{-1}) are well reproduced by the CPA, except for the loss of a few fine structures. In the optic region, the DOS is characterized by three well-defined peaks which are interpreted as due to Si-Si, Si-Ge, and Ge-Ge vibrations (in order of decreasing frequency) [10]. Some fine structures are also present, which are due to the effects of the local atomic environment (see below the discussion on the Raman activity). In this region the CPA fails not only to reproduce these fine details (which is not surprising, due to the mean-field character of the CPA), but even to predict the existence of the Si-Ge peak. The relative intensity of the Si-Si and Ge-Ge peaks is also wrong, the latter being barely visible as a shoulder on top of a structureless background.

In Fig. 2 we display the Raman cross section as obtained from SC and CPA calculations, neglecting the differences in the Si and Ge polarizabilities. In agreement with experimental findings [11], and as expected from inspection of the DOS, SC calculations predict the existence of three well-defined Raman resonances, corresponding to Si-Si, Si-Ge, and Ge-Ge vibrations. Here again, the Si-Ge peak is missing in the CPA, replaced by a featureless background, while the Ge-Ge one is barely visible. SC calculations display weak additional features between the Si-Ge and Si-Si main peaks in agreement with experiments, and a good overall agreement is found for the positions of the main as well as of the weak peaks over the whole range of compositions [12].

The weak peaks in the region between the Si-Ge and Si-Si peaks have been interpreted as due to the effect of different local atomic environments [11]. In order to put this interpretation on a firmer basis, we define a partial density of states, decomposed according to the number of X atoms (X=Si or Ge) vibrating at a given frequency and surrounded by a given number n of like atoms: $n(\omega,X_n)=\sum_\nu \delta(\omega-\omega_\nu)\sum_{i\alpha}|\xi_\nu^{i\alpha}|^2 P^i(X_n)$, where the ξ's are vibrational eigenvectors, the index i indicates the lattice position, α is the Cartesian component, and $P^i(X_n)=1$ if the ith lattice site is occupied by an X atom surrounded by n like atoms, while $P^i(X_n)=0$ otherwise.

In Fig. 3 we display $n(\omega,X_n)$ calculated for $Si_{1/2}Ge_{1/2}$. Let us concentrate on the Si_n peaks. It is easily recog-

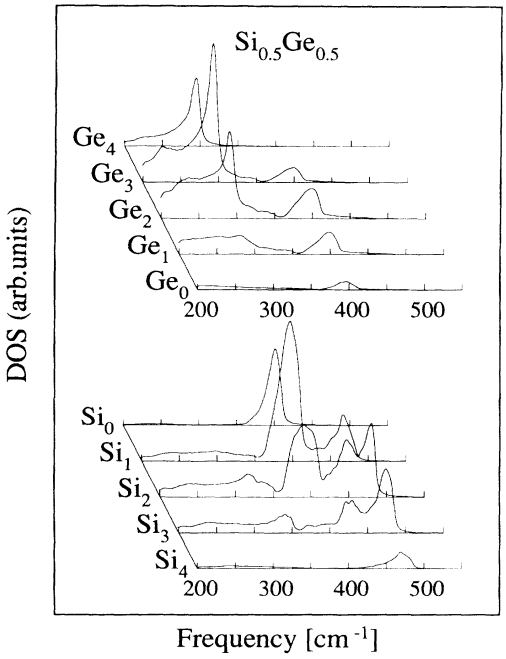

FIG. 3. Partial density of states of $Si_{1/2}Ge_{1/2}$ resolved according to the local environment (see text).

nized that different local configurations give rise to different shapes of the partial density of states, thus confirming that the weak peaks are due to local fluctuations of the atomic structure. In order to get further insight into the mechanisms which govern the positions of the weak peaks, we examine the simplest ordered structures of $Si_{1/2}Ge_{1/2}$ which display homogeneously a given local atomic configuration, and we restrict ourselves to the three highest-lying modes. These special structures are the zinc-blende (ZB) structure for Si_0, the $RH1$ structure for Si_1, the Si_2/Ge_2 (001) superlattice for Si_2, the $RH2$ structure for Si_3, and the diamond structure for Si_4. By $RH1$ and $RH2$ we indicate the two inequivalent Si_2/Ge_2 (111) superlattices which are characterized by different layer stackings: Si-Ge-Ge-Si and Si-Si-Ge-Ge for $RH1$ and $RH2$, respectively, where longer dashes correspond to larger interplanar spacings. The frequencies of superlattice modes are mainly determined by the type of bonds which stretch to first order in the phonon amplitude ("active bonds"). If one mode has only Si-Si active bonds, its frequency is very close to that of pure (strained) Si; if it has only Si-Ge active bonds its frequency is close to that of the ZB structure; if both types of bonds are active, the frequency is intermediate. The $RH1$ structure (corresponding to Si_1) has one doubly degenerate mode with only Si-Ge active bonds and a nondegenerate mode in which all the bonds are active. The (001) superlattice (corresponding to Si_2) has three distinct peaks. The lowest-lying mode has only Si-Ge active bonds; in the highest-lying mode only Si-Si bonds stretch; in the third mode all the bonds are active. The $RH2$ structure (corresponding to Si_3) has one doubly degenerate mode in which only Si-Si bonds stretch, and a nondegenerate mode where all the bonds are active. The frequency of the "intermediate" modes increases with the number of unlike atoms. All the features described above for the representative ordered structures are also found for the corresponding local environments of the bulk alloy. The importance of the local atomic environment in determining the weak peaks of the alloy had already been stressed in Ref. [11]. Contrary to what was suggested in this reference, however, our analysis shows that the same local environment can give rise to more than one weak peak, according to which bonds are active in the vibration. Also the order of the weak peaks with respect to the number of neighboring like atoms is different from what was suggested in Ref. [11].

In Fig. 4 we report the spectral density of states (SDOS) of $Si_{1/2}Ge_{1/2}$ along the Δ (Γ-X) direction, as calculated by SC's and by the CPA. In the acoustic region, lattice vibrations—both longitudinal and transverse—maintain the well-defined dispersive character they have in the pure constituents. Analogous to what happens in pure Si and Ge, the transverse branch is very flat and the longitudinal one merges in the optical region. As was the case for the total DOS, the CPA provides a qualitative correct picture of the "phonon dispersions." The

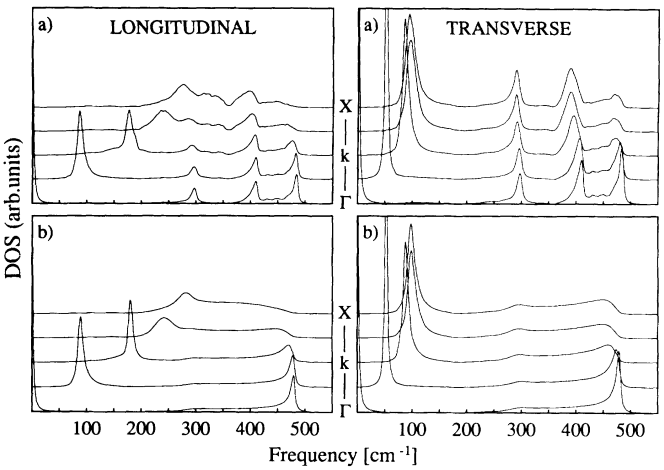

FIG. 4. Spectral density of states of $Si_{1/2}Ge_{1/2}$ along the Δ direction, as calculated from SC's (upper panels) and by the CPA (lower panels).

situation is much more complex in the optic region, where CPA and SC calculations provide qualitatively different pictures. Let us examine first the SC results. At zone center, the SDOS displays three well-defined main peaks corresponding to Si-Si, Si-Ge, and Ge-Ge vibrations. The sharpness of these structures was expected by analogy with the Raman cross section which is closely related to the zone-center SDOS (in the CPA, they would in fact coincide). This fact seems to suggest that optic phonons maintain their dispersive character despite the presence of disorder, as was the case in AlGaAs alloys [7(a),2]. This is manifestly not the case here. The longitudinal Si-Si peak loses its identity as one approaches the zone border, merging into the Si-Ge band. The Ge-Ge longitudinal peak also disappears, merging into the acoustic band near the zone border. The Si-Ge peak, on the contrary, seems to maintain its identity, though broadening as one gets off zone center. The transverse branches—which are much flatter in the pure compounds and stay further from the acoustic modes—seem to be less sensitive to disorder, and one can continue to think of a rather well-defined ω vs $\mathbf{q}$ dispersion in the bulk alloy. As one could expect, the CPA completely fails in providing even a qualitative picture of the dispersions in the optic region. The Si-Ge band is simply missing, while the Ge-Ge band is barely visible.

The origin of the failure of the CPA can be traced back to a rather general feature of the CPA, as applied to alloy lattice-dynamical calculations, which does not appear to have been properly appreciated so far. The situation is already manifest in a simple model. Consider a crystal made of weakly interacting diatomic molecules, whose constituents are atoms of species A (mass m_A) with probability x and B (mass m_B) with probability $1-x$. Suppose that the intramolecular force constant k is independent of which atoms actually form the molecule, and that the intermolecular force constants can be neglected (i.e.,

that the separations among the optical peaks of the A_2, AB, and B_2 compounds are much larger than the typical bandwidths). Under these assumptions, the average Green's function of the system is

$$\bar{g}(\omega)=\frac{x^2}{\mu_A\omega^2-k}+\frac{(1-x)^2}{\mu_B\omega^2-k}+\frac{2x(1-x)}{\mu_{AB}\omega^2-k}, \quad (1)$$

where $\mu_A=\frac{1}{2}m_A$, $\mu_B=\frac{1}{2}m_B$, and $\mu_{AB}=m_Am_B/(m_A+m_B)$. The alloy DOS clearly displays three peaks corresponding to AA, AB, and BB vibrations, at all concentrations. In the CPA, atoms in a A_xB_{1-x} alloy are assigned an effective, frequency-dependent mass which is determined by the condition that the T matrix corresponding to the substitution of a single effective mass with a physical one vanishes on the average. Applying the CPA to this simple model, one would obtain

$$g_{\mathrm{CPA}}(\omega)=\frac{1}{\mu_{\mathrm{CPA}}\omega^2-k}, \quad (2)$$

where the frequency-dependent effective mass μ_{CPA} satisfies the self-consistent equation

$$\mu_{\mathrm{CPA}}=\frac{\bar{\mu}_A\bar{\mu}_B\omega^2-k[x\bar{\mu}_A+(1-x)\bar{\mu}_B]}{[x\bar{\mu}_B+(1-x)\bar{\mu}_A]\omega^2-k}, \quad (3)$$

$$\bar{\mu}_A=\frac{2\mu_{\mathrm{CPA}}m_A}{2\mu_{\mathrm{CPA}}+m_A},\quad \bar{\mu}_B=\frac{2\mu_{\mathrm{CPA}}m_B}{2\mu_{\mathrm{CPA}}+m_B}.$$

For $x\neq\frac{1}{2}$ the CPA DOS displays a single δ-like peak at the pure-component resonance of the majority band and a broad structure centered at the mixed-compound resonance, whose width vanishes in the high- and low-concentration limits. For $x=\frac{1}{2}$, one has instead two δ-like peaks corresponding to the two pure-component resonances and the broad structure covers the entire range in between. This very simple model—which is exact in the narrow-band limit—retains the essential features of the full calculation and shows that mass disorder, though usually considered as site diagonal (and treated as such in the CPA) has in fact the same effect as off-diagonal disorder in that the vibrational properties are determined by the *bond force constant* k divided by the square root of the product of the atomic masses. In the narrow-band limit, therefore, the alloy displays as many peaks as the number of different *bonds*, even though the interatomic force constants are not affected by disorder. The CPA, instead, stresses the role of *atomic masses* and displays as many peaks as the number of different *atoms*. These considerations show why the CPA can be successful in pseudobinary alloys such as AlGaAs. In this case, the anionic sublattice is not affected by disorder and the number of different bonds is equal to the number of different cationic species on the disordered sublattice.

In this Letter we have shown that the CPA—as it is usually applied to lattice-dynamical calculations for substitutional alloys—may fail badly in predicting even the gross features of the spectrum. It is possible that cluster extensions of the CPA as well as a treatment of mass disorder as off-diagonal may contribute to overcome some of the difficulties outlined in this work. SC calculations, however, have been shown to provide a rather reliable insight into the microscopic mechanisms responsible for the observed features of substitutionally disordered systems, still requiring a computational effort which is by now affordable by a large scientific community.

This work has been partially supported by the Italian Consiglio Nazionale delle Ricerche under Grant No. 91.00943.69PF, by the European Research Office of the U.S. Army under Grant No. DAJA 45-89-C-0025, and by the Swiss National Science Foundation under Grant No. 20-5446.87.

[a]Permanent address: SISSA, via Beirut 2/4, Trieste I-34014, Italy.

[1] (a) S. Baroni, P. Giannozzi, and A. Testa, Phys. Rev. Lett. **58**, 1861 (1987); (b) P. Giannozzi, S. de Gironcoli, P. Pavone, and S. Baroni, Phys. Rev. B **43**, 7231 (1991).

[2] S. Baroni, S. de Gironcoli, and P. Giannozzi, Phys. Rev. Lett. **65**, 84 (1990).

[3] E. Molinari, S. Baroni, P. Giannozzi, and S. de Gironcoli, Phys. Rev. B **45**, 4280 (1992).

[4] S. de Gironcoli, Phys. Rev. B **46**, 2412 (1992).

[5] J. L. Beeby and S. F. Edwards, Proc. R. Soc. London A **274**, 395 (1963).

[6] P. Soven, Phys. Rev. **156**, 809 (1967); D. W. Taylor, Phys. Rev. **156**, 1017 (1967).

[7] (a) B. Jusserand, D. Paquet, and F. Mollot, Phys. Rev. Lett. **63**, 2397 (1989); (b) B. Jusserand, F. Mollot, L. G. Quagliano, G. Le Roux, and R. Planel, Phys. Rev. Lett. **67**, 2803 (1991).

[8] M. Bernasconi, L. Colombo, L. Miglio, and G. Benedek, Phys. Rev. B **43**, 14447 (1991); M. Bernasconi, L. Colombo, and L. Miglio, Phys. Rev. B **43**, 14457 (1991).

[9] S. Wilke, J. Mašek, and B. Velický, Phys. Rev. B **41**, 3769 (1990).

[10] M. A. Renucci, J. B. Renucci, and M. Cardona, in *Light Scattering in Solids*, edited by M. Balkanski (Flammarion, Paris, 1971), p. 326.

[11] M. I. Alonso and K. Winer, Phys. Rev. B **39**, 10056 (1989).

[12] S. de Gironcoli and S. Baroni, *Proceedings of the Twenty-First International Conference on The Physics of Semiconductors*, edited by X. Xide and K. Huang (World Scientific, Singapore, 1992).